

DISSOCIATION OF THE MOLECULAR ION  $H_2^+$  IN COLLISIONS WITH GASES

N. V. FEDORENKO, V. V. AFROSIMOV, R. N. IL'IN, and D. M. KAMINKER

Leningrad Physico-Technical Institute, Academy of Sciences, U.S.S.R.

Submitted to JETP editor July 29, 1958

J. Exptl. Theoret. Phys. (U.S.S.R.) **36**, 385-392 (February, 1959)

We have measured the cross section  $\sigma_{H^+}$  for proton production resulting from the dissociation of molecular hydrogen ions  $H_2^+$  in single collisions occurring in helium, argon, hydrogen and air. The energy  $T$  of the  $H_2^+$  ions varied between 5 and 180 kev. For hydrogen and helium the  $\sigma_{H^+}(T)$  curves possess two maxima, while for argon and air they rise monotonically. The angular distribution of primary 24-kev  $H_2^+$  ions scattered in argon without change of  $e/m$  was investigated as well as the angular distributions of  $H^+$  and  $H^-$  ions resulting from dissociation. It is concluded that with decrease of the distance of closest approach between the nuclei of the colliding particles the relative probability of scattering with dissociation increases.

## INTRODUCTION

IN investigations of inelastic collisions associated with changes of  $e/m$  for the molecular ion  $H_2^+$  the following possible processes must be considered:



Process (I) is ordinary charge transfer with the capture of a single electron from the target atom. Processes (II) – (VII) are different dissociation modes of the molecular ion  $H_2^+$  resulting in the formation of the atomic particles  $H^+$ ,  $H^0$ , and  $H^-$ ; (II) – (V) are dissociation processes with electron capture; (VI) is dissociation without electron transfer and (VII) is dissociation with the  $H_2^+$  ion losing an electron.

The sum of the cross sections for processes (II) – (VII) gives the total dissociation cross section  $\sigma_d$ . The cross section for proton production  $\sigma_{H^+}$  is the sum of the cross sections for the processes (III), (VI), and (VII).  $\sigma_0$ , the cross section for the production of neutral particles, is the sum of the cross sections for processes (I), (II), (IV), and (VI).  $\sigma_{H^-}$ , the cross section for the production of  $H^-$  ions, is the sum of the cross sections for processes (III), (IV), and (V).

The principal role in the dissociation of the  $H_2^+$

ion at kilovolt energies is evidently played by the processes (II), (VI), and (VII). Processes leading to the production of fast negative ions possess small cross sections.<sup>1</sup> The energy expended in each of processes (I) – (VII) varies depending on the electronic and vibrational excitation energies of the two colliding particles.

The theory of molecular ion dissociation through collisions with atoms is not highly developed. The cross sections for (VI) and (VII) at high velocities in the Born approximation have been estimated only in a brief paper by Salpeter.<sup>2</sup> Effat's experimental results,<sup>3</sup> obtained with a cyclotron, are in satisfactory agreement with Salpeter's theory. The total cross section  $\sigma_{H^+}$  for proton production from the dissociation of  $H_2^+$  ions in nitrogen, argon, neon, and hydrogen has been measured by Fedorenko<sup>4</sup> at 5 – 25 kev. Damodaran<sup>5</sup> measured  $\sigma_0$  and  $\sigma_{H^+}$  in a few gases at 100 – 200 kev. Very little information is available regarding the cross sections for  $H_2^+$  dissociation at low energies.<sup>6,7</sup>

In the present work we measured the proton-production cross sections at energies intermediate between those used in references 4 and 5, in the atomic gases helium and argon and molecular gases hydrogen and air.

## 1. DESCRIPTION OF APPARATUS

Measurements were obtained with the mass-spectrometric apparatus which was described in earlier papers by our group.<sup>8,9</sup> We shall give a brief description of the present experiment. A monoenergetic  $H_2^+$  ion beam obtained by means

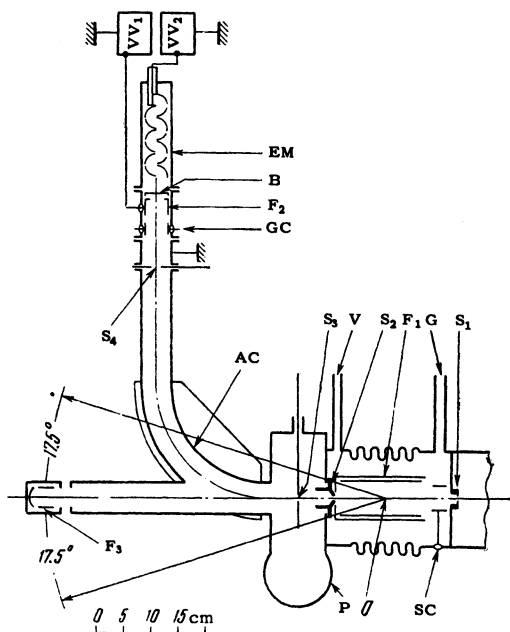


FIG. 1. Diagram of collision chamber and analyzer. AC – analyzing chamber; O – geometric center of rotation of analyzer;  $S_1$  – entrance slit of collision chamber;  $S_2$  – exit slit of collision chamber;  $S_3$  – collimating slit for investigating ion scattering;  $S_4$  – exit slit of analyzer;  $F_1$  – collector of primary ions;  $F_2$  – collector of analyzer;  $F_3$  – collector of fast neutron particles; B – bottom of collector  $F_2$ ; EM – electron multiplier;  $VV_1$  and  $VV_2$  – vacuum-tube voltmeters; GC – guard condensers; P – diffusion pump; G and V – tubes for gas inlet and vacuum gauge connection.

of a magnetic monochromator entered a collision chamber filled with the investigated gas and was subjected to  $e/m$  analysis in the magnetic field. The primary beam entering the collision chamber possessed initial divergence less than  $0.5^\circ$  in both the horizontal and vertical directions. A schematic horizontal section of the collision chamber and analyzer are shown in Fig. 1. For investigations of ion scattering the analyzer can be rotated around a vertical axis passing through the geometric center of the collision chamber through the angular range  $-17.5^\circ < \theta < 17.5^\circ$  from the primary-beam direction. The entrance slit  $S_1$  of the collision chamber was 1 mm wide and 3 mm long. Slits  $S_2$  and  $S_3$  served for collimation of scattered ion beams. The analyzer was rotated and the widths of the slits were varied without affecting the vacuum. Variation of the magnetic field strength in the analyzer can be used to send to collector  $F_2$  either primary  $H_2^+$  ions or  $H^+$  and  $H^-$  ions resulting from  $H_2^+$  dissociation in the collision chamber. The adjustable slit  $S_4$  was used to determine the geometric widths of spectral lines, which were considerably smaller than the inlet aperture of collector  $F_2$ . The current to  $F_2$  was measured by a vacuum-tube voltmeter of sensitivity  $1 \times 10^{-14}$  amp

per scale division. Sensitivity was increased by the use of a measuring scheme which consisted of an open electron multiplier connected to the input of a vacuum-tube voltmeter; the sensitivity of this system was  $1 \times 10^{-17}$  amp per division. For the measurement of very small currents the bottom of  $F_2$  was raised by means of flexible bellows and the ion beam entered the electron multiplier. A similar measuring scheme was previously used by the authors of the present paper to investigate the scattering of secondary ions<sup>10</sup> and in the present instance was used to investigate the scattering of fast ions. The primary beam passing through the collision chamber was measured by  $F_1$  with rotation of the analyzer through the angle  $\theta = \pm 5^\circ$ , in which position practically the entire primary beam was captured by  $F_1$ . The primary current of  $1 \times 10^{-8} - 1 \times 10^{-6}$  amp was measured by a galvanometer. Collector  $F_3$  was used to detect fast neutral particles produced from  $H_2^+$  ions.

## 2. INVESTIGATION OF SCATTERING

For the investigation of scattering we used a procedure similar to that described in references 11 and 12. The first collimating slit  $S_2$  was 1.5 mm wide and 6 mm long; the dimensions of the second collimating slit  $S_3$  were 0.25 and 2.0 mm, respectively. The angular resolution of the measuring scheme as a whole was  $\sim 2.3^\circ$ .

After the collision chamber was filled with gas we observed some broadening of primary  $H_2^+$  ion lines and the appearance of atomic  $H^+$  and  $H^-$  ions resulting from  $H_2^+$  dissociation. We investigated (1) the angular distribution of primary  $H_2^+$  ions with the collision chamber pumped down to its ultimate vacuum, i.e., the shape of the beam; (2) the angular distribution of  $H_2^+$  ions and the angular distributions of  $H^+$  and  $H^-$  ions after the collision chamber was filled with gas. For each case separately we determined the angular distribution

$$f(\theta) = i_2 / i_1, \quad (1)$$

where  $\theta$  is the angle of ion deflection due to rotation of the analyzer,  $i_1$  is the primary current in the collision chamber and  $i_2$  is the current to  $F_2$ . We used the data to compare the angular distributions for  $H_2^+$ ,  $H^+$  and  $H^-$  obtained with completely identical geometry.

## 3. TOTAL CROSS SECTIONS $\sigma_{H^+}$ FOR PROTON PRODUCTION

Preliminary scattering experiments showed that a large fraction of the protons resulting from  $H_2^+$  dissociation are deflected through small angles

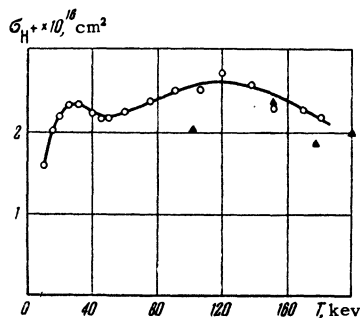


FIG. 2. Proton production cross section in helium as a function of  $H_2^+$  energy;  $\Delta$  - data from reference 5.

from the primary beam direction. Therefore, as in references 4, 5, and 8,  $\sigma_{H^+}$  was determined by means of a collision chamber with a wide entrance slit. The second collimating slit  $S_3$  was removed and the width of slit  $S_2$  was increased to 4.5 mm. It was determined experimentally that further increase of the slit width does not produce an appreciable increase of the proton current to  $F_2$ . For the measurement of  $\sigma_{H^+}$  the analyzer was set in the position  $\theta = 0^\circ$ . Proton production cross sections were determined from the formula

$$\sigma_{H^+} = i_2 / i_1 n l k, \quad (2)$$

where  $n$  is the atomic concentration of the given gas in the collision chamber;  $i_2$  is the proton current measured by  $F_2$ ;  $i_1$  is the primary  $H_2^+$  ion current in the collision chamber;  $l$  is the length of the collision chamber (16 cm);  $k$  is the so-called "penetration coefficient" of the analyzer, which is the ratio of primary beam currents measured by  $F_2$  and  $F_1$  when the collision chamber is filled with gas. The value of  $k$  characterizes the attenuation of the primary ion beam through elastic and inelastic scattering; in our work  $k$  varied from 0.85 to 0.95. The conditions for single collisions between primary ions and gas ions, resulting in dissociation, were established by investigating the ratio  $i_2/i_1 = \varphi(p)$  for protons entering  $F_2$ . The principal measurements were obtained at the pressure  $p \approx 1.5 \times 10^{-4}$  mm over a linear portion of this relation. Differential pumping maintained the pressure below  $5 \times 10^{-6}$  mm in other portions of the apparatus.

The purity of the investigated gas was monitored

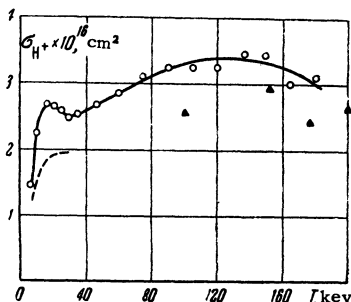


FIG. 4. Proton production cross section in hydrogen as a function of  $H_2^+$  energy  $\Delta$  - data from reference 5; dashed line - curve from reference 4.

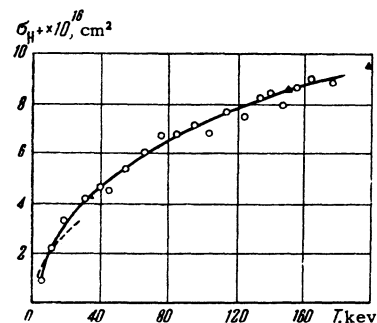


FIG. 3. Proton production cross section in argon as a function of  $H_2^+$  energy;  $\Delta$  - data from reference 5; dashed line - curve taken from reference 4.

by a separate analyzer, which was previously used to investigate the charges of secondary ions produced through the ionization of gas atoms by the ion beam.<sup>13</sup> Random errors in determining  $\sigma_{H^+}$  are estimated at  $\pm 12\%$ , combining errors in measuring the gas pressure ( $\pm 6\%$ ) and the ion current ( $\pm 6\%$ ).

Equation (2) was also used to determine  $\sigma_{H^-}$ , but we regard the value obtained for the latter as approximate since the  $\sigma_{H^-}(p)$  curve did not possess a well-defined linear portion.

## 4. EXPERIMENTAL RESULTS AND DISCUSSION

### 1. Proton and $H^-$ Production Cross Sections

The dependences of  $\sigma_{H^+}$  on  $H_2^+$  ion energy in helium, argon, hydrogen, and air are shown in Figs. 2, 3, 4, and 5. The cross sections were calculated for a single primary molecular ion per gas molecule. All of the figures also show the values of  $\sigma_{H^+}$  taken from Damodaran's data<sup>5\*</sup> and Figs. 3, 4, and 5 give the corresponding curves taken from Fedorenko's work.<sup>4</sup> All of the experimental data for argon show satisfactory consistency, whereas for the other gases the spread of experimental results somewhat exceeds the limits of the random-measurement errors indicated in the respective papers. The curves obtained in the present work give higher values of the cross sections for a single  $H_2^+$  energy. We note that in reference 4 the penetration coefficient of the analyzer did not exceed 0.35, so that, as indicated in the present work, the values of  $\sigma_{H^+}$  could be too low. The same inadequacy of the experimental procedure could have existed in reference 5 because of the relatively narrow entrance slit of the collision chamber.

It is evident from Figs. 3 and 5 that  $\sigma_{H^+}$  in argon and air increases continuously over the en-

\*Using the data of reference 5,  $\sigma_{H^+}$  can be determined from the ratio  $\sigma_{H^+}/\sigma_d$ . However, in determining the total dissociation cross section  $\sigma_d$  in reference 5 the experimental data are interpreted inaccurately, since the author neglects the possibility that  $H_2^0$  molecules resulting from ordinary charge transfer can enter the neutral-particle detector together with  $H^0$  atoms.

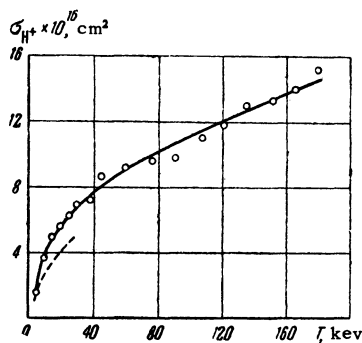


FIG. 5. Proton production cross section in air as a function of  $H_2^+$  energy;  $\Delta$  — data from reference 5 for nitrogen; dashed line — curve from reference 4 for nitrogen.

tire investigated energy range. For hydrogen and helium  $\sigma_{H^+}(T)$  shows a broad peak between 100 and 160 keV. Also, the same curves reveal an additional narrow peak, at  $\sim 15$  keV for hydrogen and  $\sim 30$  keV for helium. These narrow peaks are not very sharply defined and in general fall within the limits of error mentioned above. However, frequent repetition of measurements in this range confirmed without exception the existence of these peaks of  $\sigma_{H^+}(T)$  for hydrogen and helium.

The cross section for the production of negative ions was measured only in argon, giving  $\sigma_{H^-} \approx 1.6 \times 10^{-18}$  cm<sup>2</sup> at 12 keV. A rapid continuous reduction of  $\sigma_{H^-}$  is observed as the energy is increased up to 180 keV.

According to general theoretical concepts, the dissociation of molecular ions possessing energies of thousands of volts in collisions with atoms should proceed mainly through electron transitions to excited levels, observing the Franck-Condon principle. Dissociation due to the excitation of vibrational states plays an essential part at lower energies. It is known from the most recent work on the ionization of atoms by ionic impact<sup>8,14-17</sup> that in the kilovolt range ionization cross sections in heavy gases can attain values  $\sim 1 \times 10^{-15}$  cm<sup>2</sup> and the excitation of both colliding particles is observed. Therefore large cross sections for the dissociation of the molecular ion  $H_2^+$  are not unexpected.

It appears to us that some characteristics of the  $\sigma_{H^+}(T)$  curves can be explained qualitatively from a consideration of the theoretical potential energy curves for electron states of  $H_2^+$ .<sup>18</sup> The narrow first peak of the  $\sigma_{H^+}$  curves for hydrogen and helium can be attributed to a transition from  $^2\Sigma_g$ , the ground state of  $H_2^+$ , to the repulsive state  $^2\Sigma_u$ , with the production of a proton and of a hydrogen atom in an unexcited state. The broad second peak, at a higher energy, can be associated with a transition of  $H_2^+$  to various excited states or to a fully ionized state with the production of two protons and an electron. The cross sections  $\sigma_{H^+}$  in argon and air are considerably larger than in hydrogen and helium; this apparently results from the rela-

tively large probability of  $H_2^+$  excitation in passing through the complex electron cloud of a target atom.

## 2. Angular Distributions

In the light gases hydrogen and helium  $H_2^+$  ions with energies  $T \gtrsim 100$  keV are scattered without dissociation, and the atomic ions  $H^+$  and  $H^-$  resulting from the dissociation are deflected very little from the primary beam direction. We shall therefore give only the clearest data for scattering in argon at 24 keV, the curves for which are shown in Fig. 6. A logarithmic scale is used for the angular distribution  $f(\theta)$ .

The angular distribution curves were compared more conveniently by making them coincide at  $\theta = 0^\circ$ . The small amount of broadening of the  $H_2^+$  angular distribution for a gas-filled collision chamber is evidence that  $H_2^+$  ions are scattered without change of  $e/m$ . It is quite evident that the angular distributions of  $H^+$  and  $H^-$  ions resulting from dissociation are flatter. Similar results were previously obtained by Fedorenko<sup>11</sup> in a study of  $N_2^+$  scattering in neon and of  $H_2^+$  and  $H_3^+$  scattering in krypton.

These results permit the general conclusion that the relative probability of scattering with dissociation increases with reduction of the distance of closest approach between a molecular ion and gas atom. This conclusion is supported by the following considerations. Classical concepts can be used to interpret data on the scattering of atomic particles at kilovolt energies outside of the small-

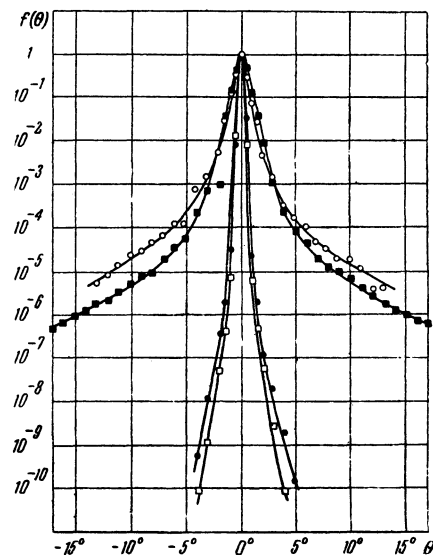


FIG. 6. Angular distributions:  $\square$  — for primary  $H_2^+$  ions, with the collision chamber at a pressure of  $5 \times 10^{-6}$  mm;  $\bullet$ ,  $\blacksquare$ ,  $\circ$  — for  $H_2^+$ ,  $H^+$  and  $H^-$ , with the collision chamber filled with argon at  $1.5 \times 10^4$  mm.

angle region.<sup>10-12,19,20</sup> Specifically, increase of the deflection angle corresponds to reduction of the impact parameter and of the distance of closest approach of the colliding particles. In addition, elastic and inelastic scattering angles differ very little when the inelastic energy loss is small compared to the kinetic energy of relative motion of the colliding particles.

The two atomic particles resulting from the dissociation of  $H_2^+$  during their separation acquire additional kinetic energy as the  $H_2^+$  ion makes its transition to a repulsive state; however this energy does not exceed 10 eV per particle even when two protons are produced. The magnitude of the additional energy can be used to determine a corresponding change of direction, which in our case is computed to be less than  $1.6^\circ$ . Therefore the different shapes of the angular distribution curves in Fig. 6 cannot be attributed only to mutual repulsion of the atomic particles produced by dissociation. Indeed, it is evident that as the deflection angle is varied a redistribution of the relative probabilities of different types of scattering is observed. Inelastic scattering with dissociation becomes relatively more probable as  $\theta$  increases. Ionic scattering without dissociation, which is elastic when unaccompanied by excitation, occurs principally at small angles.

In our earlier studies of primary ion scattering with the loss of electrons,<sup>12</sup> and of the scattering of secondary ions derived from gas atoms,<sup>17</sup> it was determined that a reduction of the distance of closest approach of the colliding nuclei is accompanied by increased relative probability of inelastic processes requiring the expenditure of relatively large amounts of energy. The results of the present work show that this phenomenological law can evidently be extended to the dissociation of molecular ions and we presume that it is a general property of atomic collisions.

In conclusion it is a pleasant obligation to thank O. B. Firsov and V. M. Dukel'skiĭ for discussions.

<sup>1</sup>Fogel', Krupnik, and Ankudinov, J. Tech. Phys. (U.S.S.R.) **26**, 1208 (1956), Soviet Phys. JTP **1**, 1181 (1956).

<sup>2</sup>E. E. Salpeter, Proc. Phys. Soc. (London) **A63**, 1295 (1950).

<sup>3</sup>K. E. A. Effat, Proc. Phys. Soc. (London) **A65**, 433 (1952).

<sup>4</sup>N. V. Fedorenko, J. Tech. Phys. (U.S.S.R.) **24**, 769 (1954).

<sup>5</sup>K. K. Damodaran, Proc. Roy. Soc. (London) **A239**, 382 (1957).

<sup>6</sup>Lamar, Samson, and Compton, Phys. Rev. **48**, 886 (1935).

<sup>7</sup>S. E. Kupriyanov and V. K. Potapov, J. Exptl. Theoret. Phys. (U.S.S.R.) **33**, 311 (1957), Soviet Phys. JETP **6**, 244 (1958).

<sup>8</sup>D. M. Kaminker and N. V. Fedorenko, J. Tech. Phys. (U.S.S.R.) **25**, 1843 (1955).

<sup>9</sup>N. V. Fedorenko, Proceedings of the Third International Conference on Ionization Phenomena in Gases, Venice, 1957, p. 295.

<sup>10</sup>V. V. Afrosimov and N. V. Fedorenko, J. Tech. Phys. (U.S.S.R.) **27**, 2573 (1957), Soviet Phys. JTP **2**, 2391 (1957).

<sup>11</sup>N. V. Fedorenko, J. Tech. Phys. (U.S.S.R.) **24**, 784 (1954).

<sup>12</sup>D. M. Kaminker and N. V. Fedorenko, J. Tech. Phys. (U.S.S.R.) **25**, 2239 (1955).

<sup>13</sup>N. V. Fedorenko and V. V. Afrosimov, J. Tech. Phys. (U.S.S.R.) **26**, 1941 (1956), Soviet Phys. JTP **1**, 1872 (1956).

<sup>14</sup>N. V. Fedorenko, J. Tech. Phys. (U.S.S.R.) **24**, 2113 (1954).

<sup>15</sup>Fedorenko, Afrosimov and Kaminker, J. Tech. Phys. (U.S.S.R.) **26**, 1929 (1956), Soviet Phys. JTP **1**, 1861 (1956).

<sup>16</sup>H. B. Gilbody and J. B. Hasted, Proc. Roy. Soc. (London) **A240**, 382 (1957).

<sup>17</sup>V. V. Afrosimov and N. V. Fedorenko, J. Tech. Phys. (U.S.S.R.) **27**, 2557 (1957), Soviet Phys. JTP **2**, 2378 (1957).

<sup>18</sup>H. S. W. Massey and E. H. S. Burhop, Electronic and Ionic Impact Phenomena (Oxford, 1952), Russ. Transl., Moscow, 1958.

<sup>19</sup>Carbone, Fuls, and Everhart, Phys. Rev. **102**, 1524 (1956).

<sup>20</sup>O. V. Firsov, J. Exptl. Theoret. Phys. (U.S.S.R.) **34**, 447 (1958), Soviet Phys. JETP **7**, 308 (1958).